Renewable Energy 74 (2015) 940–947

Contents lists available at ScienceDirect

Renewable Energy

journal homepage: www.elsevier.com/locate/renene

Thermoelectric figure of merit of bulk $FeSi_2$–$Si_{0.8}Ge_{0.2}$ nanocomposite and a comparison with β-$FeSi_2$

Milad Mohebali [a, 1], Yin Liu [a, 1], Lobat Tayebi [b, c], Jerzy S. Krasinski [a], Daryoosh Vashaee [d, *]

[a] Helmerich Advanced Technology Research Center, School of Electrical and Computer Engineering, Oklahoma State University, Tulsa, OK 74106, USA
[b] Helmerich Advanced Technology Research Center, School of Material Science and Engineering, Oklahoma State University, Tulsa, OK 74106, USA
[c] School of Chemical Engineering, Oklahoma State University, Stillwater, OK 74078, USA
[d] Department of Electrical and Computer Engineering, North Carolina State University, Raleigh, NC 27606, USA

ARTICLE INFO

Article history:
Received 26 January 2014
Accepted 21 August 2014
Available online 2 October 2014

Keywords:
Thermoelectric
Nanocomposite
Iron disilicide
Silicon germanium

ABSTRACT

Among various thermoelectric (TE) materials, iron disilicide ($FeSi_2$) has relatively low cost and non-toxic characteristics which make it appropriate for large scale applications. To enhance the dimensionless figure of merit (ZT) of this material, a composite of $FeSi_2$–$Si_{0.8}Ge_{0.2}$ with high fraction of α-$FeSi_2$ was prepared by mechanical alloying and sintering. The process was followed by thermal annealing to transform α to β phase $FeSi_2$ through a slow peritectoid reaction (several hours). The thermoelectric properties were significantly improved upon the completion of the phase transformation. At temperatures above 900 °C, $FeSi_2$ component rapidly changed from β to α phase (several minutes) leading to sudden increase of the thermal conductivity. For comparison, the thermoelectric alloy of β-$FeSi_2$ was prepared through a similar process. The effect of sintering conditions and annealing time were studied and a comparison was drawn between the thermoelectric properties of β-$FeSi_2$ and $FeSi_2$–$Si_{0.8}Ge_{0.2}$ nanocomposite. Overall, $(FeSi_2)_{0.75}(Si_{0.8}Ge_{0.2})_{0.25}$ showed 170% enhancement in ZT compared with β-$FeSi_2$ making it suitable for medium to high temperature applications (500 °C –850 °C).

1. Introduction

The era of global energy crisis and the urge to find efficient energy harvesting technologies have attracted much attention towards thermoelectric (TE) technology. Recently, there has been increasing interest in TE technology for applications including power generation, cooling, or sensing and imaging which has resulted in the development of new materials, devices, and characterization techniques [1–4]. Resulted from continuous efforts for enhancing the efficiency of TE materials, several methods based on low dimensional structures [5,6], nanostructuring [7–11], energy filtering techniques [12–14], resonant energy levels [15], embedded nanoinclusions [16–19] and complex material systems [20–22] have been developed and applied to several material systems.

The efficiency of TE materials in energy conversion is evaluated by their dimensionless TE figure of merit, $ZT = (S^2\sigma/k)T$, where Z is the figure of merit, T is the absolute temperature, S is the Seebeck coefficient, σ is the electrical conductivity, and k is the thermal conductivity. ZT is temperature dependent and each TE material is good for a certain range of working temperature.

There are several material systems that have shown improved TE properties at medium to high temperature. Among these materials, several different silicide alloys have been identified and investigated [23–27]. For example, the beta phase iron disilicide (β-$FeSi_2$) is a known TE material for medium temperature range (500 °C-900 °C) due to its thermal stability, oxidation resistance and good mechanical strength, along with low cost and non-toxicity of its raw materials [28,29]. However, despite its relatively high power factor, it has a low figure of merit [30–32]. The largest ZT reported for this material system is around $ZT = 0.25$ [30], which is too small to make an efficient device.

Thermoelectric β-$FeSi_2$ is an intrinsic semiconductor, and different dopants like Co [30] or B, and Cr [33], Ti, Nb, Zr [34], Mn [35] or Al [36] etc. are added intentionally to induce n-type or p-type characteristics, respectively, and improve its thermoelectric properties. Nanostructuring is another technique which helps increasing the ZT in TE materials by decreasing thermal conductivity through enhanced phonon scattering at the nanocrystals

* Corresponding author. Tel.: +1 919 515 9599.
E-mail addresses: daryoosh.vashaee@ncsu.edu, daryoosh.vashaee@okstate.edu, vashaee@gmail.com (D. Vashaee).
[1] These authors contributed equally to this work.

http://dx.doi.org/10.1016/j.renene.2014.08.059
0960-1481/

Table 1
Powder preparation parameters.

Powder	Composition	Milling machine	Milling time (hr)	Bowl and ball material
$FeSi_2$	$(Fe_{0.95}Co_{0.05})Si_2$	Vibratory mill	96	Stainless steel
SiGe	$Si_{0.775}Ge_{0.2}P_{0.025}$	Planetary ball mill	56	Tungsten carbide
$FeSi_2$–SiGe	$(FeSi_2)_{0.75}(Si_{0.8}Ge_{0.2})_{0.25}$	Planetary ball mill	30	Tungsten carbide

Table 2
Preparation properties of samples 1–4.

Sample ID	Pressure (MPa)	Temperature (°C)	Time (min)
1	120	1150	6
2	120	1000	6
3	120	1100	6
4	120	1100	15

interfaces [37]. In order to further improve the thermoelectric performance of β-$FeSi_2$, several additives have been investigated to form a nanocomposite of $FeSi_2$ [38–40]. Sm_2O_3 and Er_2O_3 containing $FeSi_2$ have shown a ZT of 0.54 and 0.56 respectively at approximately 650 °C [38].

The thermoelectric β-$FeSi_2$, with orthorhombic structure, forms through a peritectoid reaction from the high temperature tetragonal α-Fe_2Si_5 and cubic ε-FeSi phases [41]. This peritectoid reaction is very slow for β-$FeSi_2$ formation. Since the reaction is controlled by diffusion through the solid β-phase shell by the peritectoid reaction, the transforming rate from β to α is much lower than α to β [42]. Therefore, a long-time annealing after the sintering is usually required to obtain dominant phase of β in an α-$FeSi_2$.

$Si_{1-x}Ge_x$ (SiGe) alloys have been the principal thermoelectric materials for power generation at high temperatures ($T > 1100$ °C). SiGe alloys possess high mechanical strength, high melting point, low vapor pressure and resistance to atmospheric oxidation [43,44]. The ZT of p-type and n-type SiGe in Radioisotope Thermoelectric Generators (RTG) are ~0.5 and ~0.9 at 825 °C, respectively [45]. The maximum reported ZT for p-type bulk nanostructure $Si_{0.8}Ge_{0.2}$ and n-type bulk nanostructure $Si_{0.8}Ge_{0.2}$ are ~0.9 [46,48] and ~1.3 [47], respectively. The typical content of germanium in SiGe TE alloy is about 20%. It is highly desired though to reduce this amount due to the high cost of germanium.

In order to increase the low thermoelectric efficiency of $FeSi_2$ without significant increase in the cost of the starting materials, a nanocomposite of $FeSi_2$ and SiGe was prepared by mechanical alloying, sintering, and subsequent annealing. Hot-press conditions for sintering of the samples were also investigated, and finally, a comparison was made between the pure $FeSi_2$ and $FeSi_2$–$Si_{0.8}Ge_{0.2}$ composites.

2. Materials and methods

Elemental Si (purity > 99.9%), Ge (purity > 99.9%), Fe (purity > 99.9%), Co (purity > 99.9%), and P (purity > 99.9%) were used to prepare Co-doped $FeSi_2$ and P-doped $Si_{0.8}Ge_{0.2}$ powders for making the final $FeSi_2$–$Si_{0.8}Ge_{0.2}$ composite. The milling conditions for $FeSi_2$, SiGe and $FeSi_2$–SiGe composite powders are summarized in Table 1.

$FeSi_2$–SiGe composite powder was then loaded into a graphite die of 12.7 mm ID and sintered with a homemade DC hot-press compaction system under different conditions provided in Table 2. The density of the samples was measured by the Archimedes' method, and all the samples had a density of ~95% of the nominal density.

An argon atmosphere furnace was used to anneal the samples. The samples were cut into different shapes for characterization. Milled powders and sintered samples were characterized by a Bruker AXS D8-Discover X-Ray Diffraction (XRD) machine. Phase identification and crystallite size analysis were performed by XRD spectrum collected using CuKα radiation at 40 kV and 40 mA. The Seebeck coefficient and electrical conductivity of the samples were measured simultaneously through a four-probe method by means of commercially available equipment (Ulvac, ZEM-3). Thermal conductivity was measured by a laser flash apparatus (Netzsch LFA 457). The uncertainty of the measurements for thermal conductivity, electrical conductivity and Seebeck coefficient measurements were ~10%, 5%, and 5%, respectively. The structures of the sintered samples were studied by scanning electron microscopy (Hitachi S4800) investigations of the cleaved surfaces of the samples.

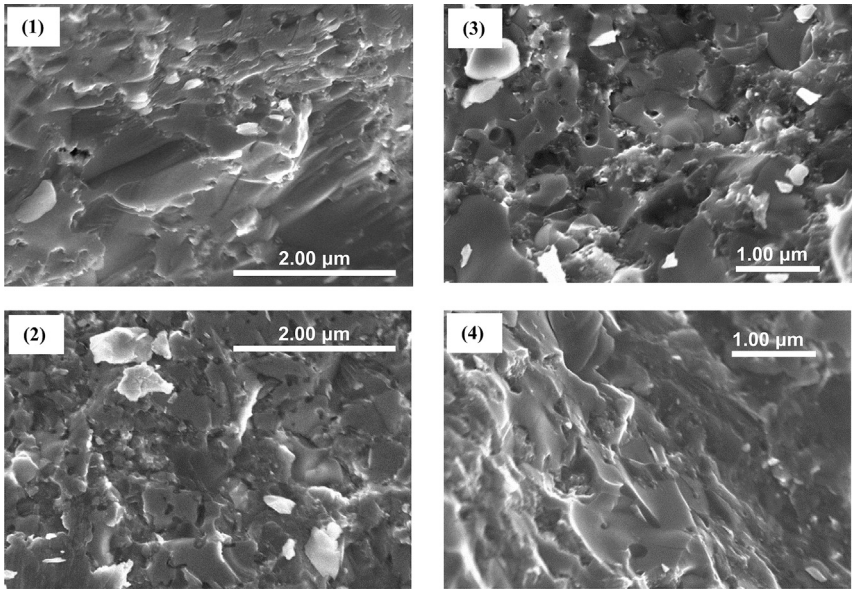

Fig. 1. SEM images of samples 1, 2, 3 and 4 in their as-pressed form.

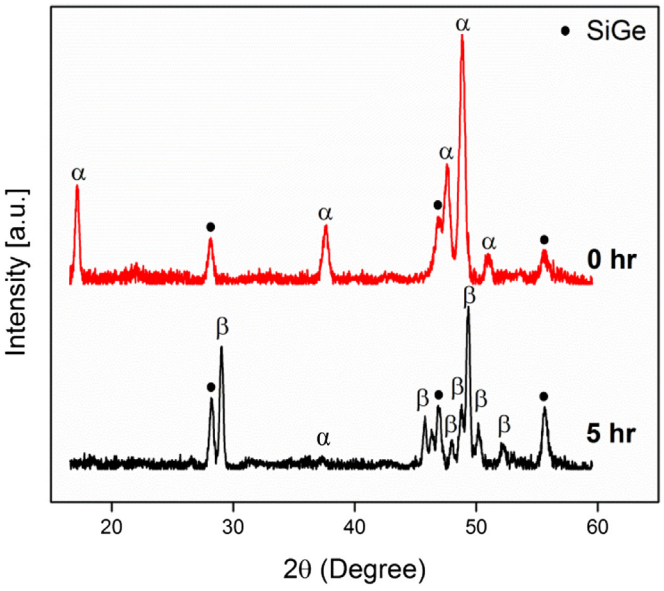

Fig. 2. XRD patterns of sample 1 in as-pressed form and after 5 h of annealing at 850 °C.

3. Results and discussion

Fig. 1 shows the SEM images from the hot pressed samples. Particle size increases by increasing hot press temperature from sample 2 with the smallest particle size, to sample 3 and then 1. The porosity follows the reverse order, decreasing by increasing temperature. Comparing sample 3 and 4, it can be concluded that increasing the holding time at high temperatures increases the particle size and reduces the porosity.

Sample 1 was selected as the study sample to investigate the phase evolution of the $FeSi_2$–SiGe composite during the annealing process. Fig. 2 shows the XRD patterns of sample 1 right after hot-pressing, and after 5 h of annealing at 850 °C. After hot-pressing, the sample consists of α-$FeSi_2$ and SiGe, while after 5 h of annealing, a significant fraction of α-Fe_2Si_5 and ε-FeSi have transformed into the β-$FeSi_2$ phase. Phosphorous doped $Si_{0.8}Ge_{0.2}$ is recognized in XRD patterns by Si peaks which are shifted to a certain amount toward higher d-spacings, meaning that bigger sized Ge atoms have been placed in the Si unit cells expanding the planar distances.

Thermoelectric properties of sample 1 in its original hot-pressed form and after being annealed at 5, 10 and 15 h at 850 °C are given in Fig. 3. The original sample shows the typical metallic high electrical and thermal conductivities, and low

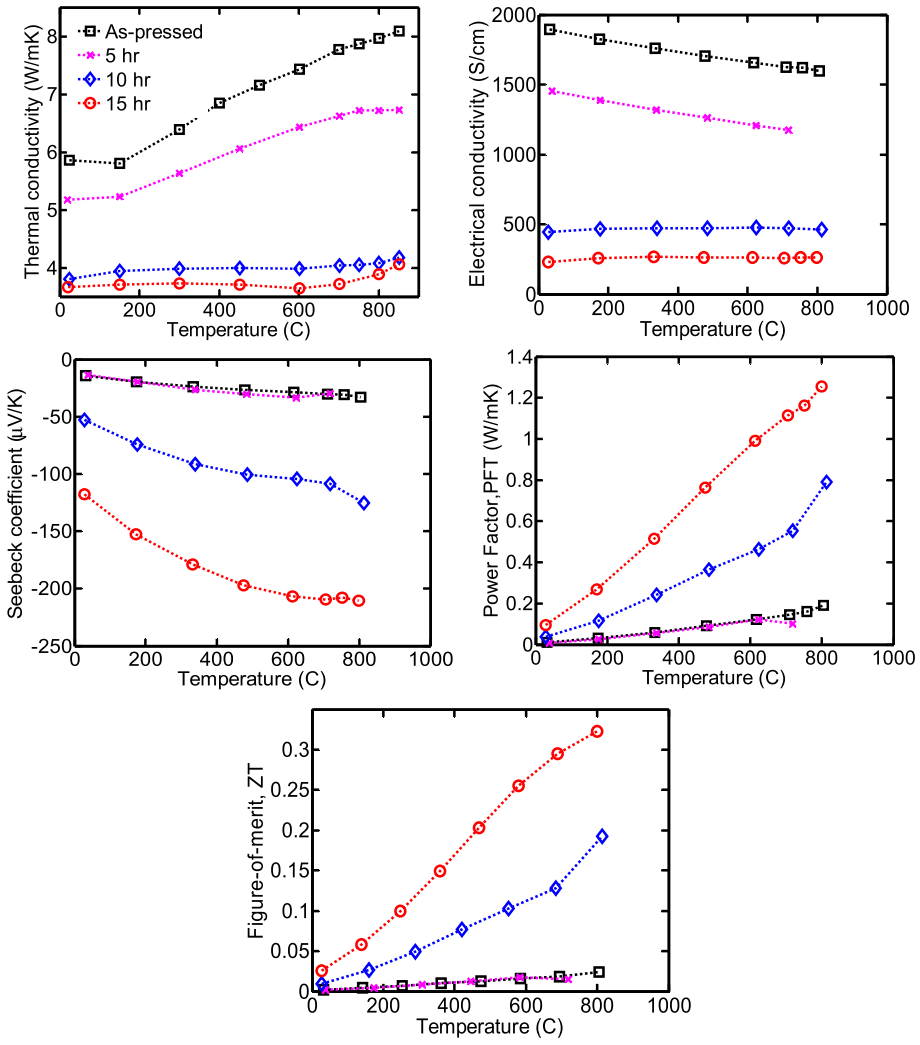

Fig. 3. Thermoelectric properties of the composite sample sintered at 1150 °C for 6 min (sample 1) before annealing and after annealing at 850 °C for 5, 10 and 15 h.

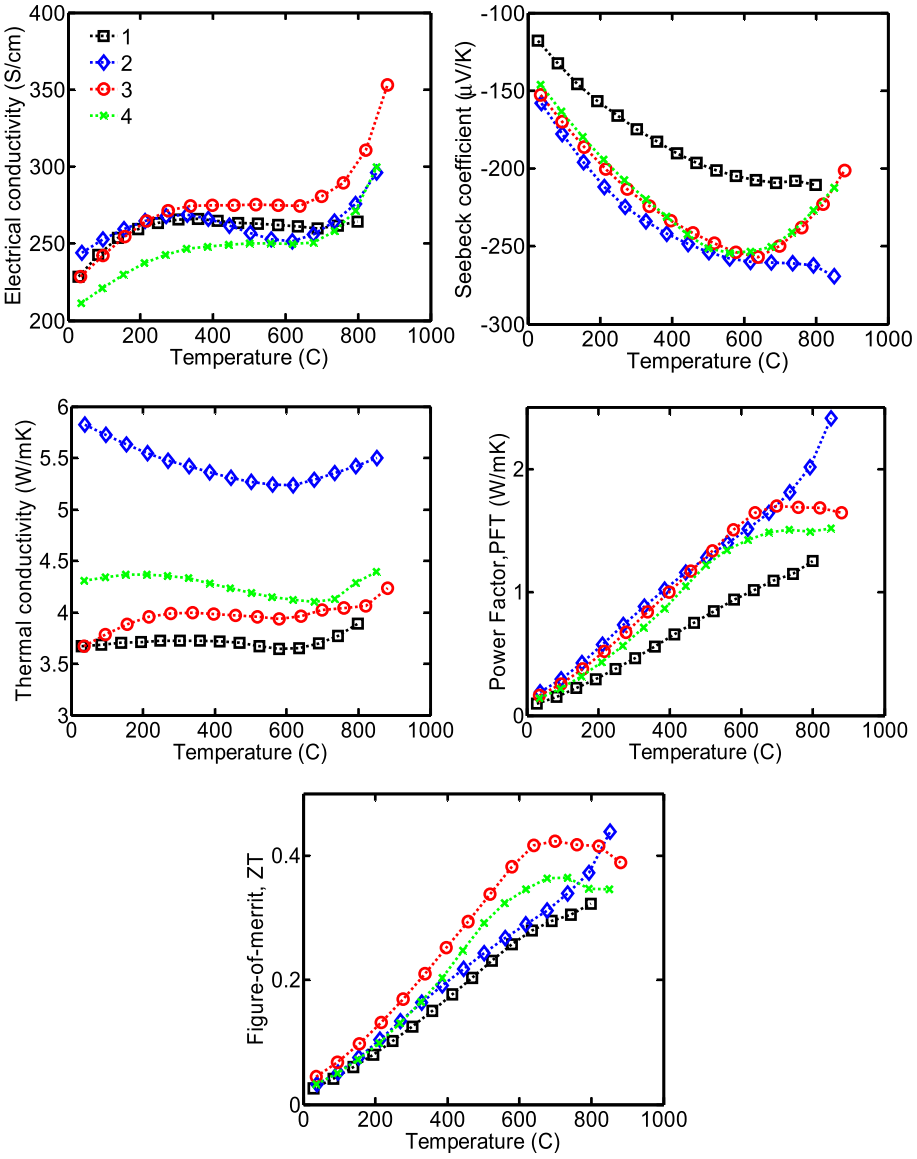

Fig. 4. Thermoelectric properties of samples sintered under different hot-press conditions and after annealing at 850 °C for 15 h. Sample 2 which was sintered at 1100 °C for 6 min shows the highest ZT among all samples.

Seebeck coefficient and low ZT. The short version "Figure of merit, ZT" was used as labels in all the graphs instead of the "dimensionless figure of merit, ZT". Annealing for 5 h did not show significant improvement in the product of PF and temperature (PFT) or the ZT, but showed reductions in electrical and thermal conductivity values. Being consistent with the XRD results, these changes indicate that the phase transformation has already started, but the major phase is still the alpha phase. The increase of the annealing time to 10 and 15 h resulted in a concomitant increase in Seebeck coefficient, PFT and ZT. The electrical conductivity reduced with the beta phase formation at 5 h, and reduced even more after annealing for 10 h. However, the Seebeck coefficient showed only a small enhancement after 5 h of annealing, but then reduced more and more as the annealing continued. Further annealing up to 15 h did not result in further decrease of thermal conductivity. The samples were also tested under cooling cycles, heating the sample from room temperature to 850 °C and cooling back to room temperature with heating/cooling rate of approximately 5 °C/min. In contrast to SiGe, the properties of our samples were well reproducible after several heating/cooling cycles indicating no dopant precipitation [48,49].

Samples 2–4 were annealed at 850 °C for 15 h and thermoelectric properties were measured as given in Fig 4. Sample 2 showed the highest value of ZT among these samples. The trends can be understood as both thermal conductivity and electrical conductivity are very sensitive to crystallite size and porosity as well as the interplay of these two parameters. Both hot-press temperature and holding time affect the final ZT of the material. It is thus interesting that even though sample 2 and 3 are more porous compared to sample 1 and 4, yet they possess higher ZT, meaning that crystallite size plays a major role in the thermoelectric properties of the composite structure. Sample 4 which was held at 1100 °C for 15 min showed better ZT that sample 1 treated at 1150 °C for 6 min, which indicates that the hot-press temperature must be optimized versus the holding time for better final properties.

Another important aspect affecting the final thermoelectric properties is the peritectoid reaction that takes place during

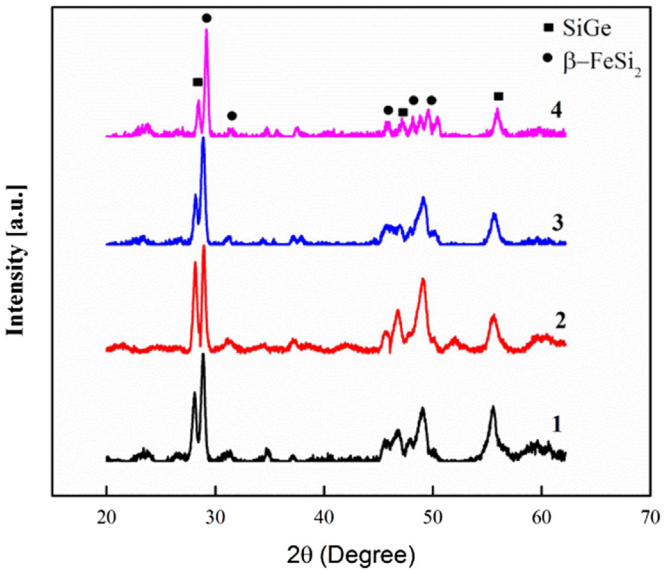

Fig. 5. XRD pattern of samples 1–4 after annealing at 850 °C for 15 h.

annealing to form the thermoelectric beta phase material. The anticipated lower crystallite size of the sample treated at lower hot-press temperature would result in more nucleation sites for the beta phase whose growth is controlled by diffusion [42]. Thus, the sample with smaller crystallite size should have higher concentration of beta phase formed at a given amount of annealing time, consistent with a considerably higher Seebeck coefficient observed for sample 2 compared to the rest of the samples (Fig. 5).

Sample 2 which showed the highest ZT value among all the samples was then annealed for longer time periods to find the optimum annealing time which would result in the highest ZT. Fig. 6 shows the change in ZT of sample 2 after annealing in 850 °C for 15, 20, 25, 30 and 45 h. It can be seen that the ZT is increased up to ~0.54 at 714 °C and 0.45 at 850 °C after 20 h annealing. However, further increase in annealing time reduced the ZT. Therefore the optimum annealing time to gain a high ZT from the $FeSi_2$–$Si_{0.8}Ge_{0.2}$ composite is approximately 20 h.

The ZT value of 0.54 is more than twice the highest reported ZT value for $FeSi_2$ alone (ZT = 0.22), making this material a better choice for energy harvesting applications. It is also noticeable that the value of ZT remains above 0.4 for the entire temperature range

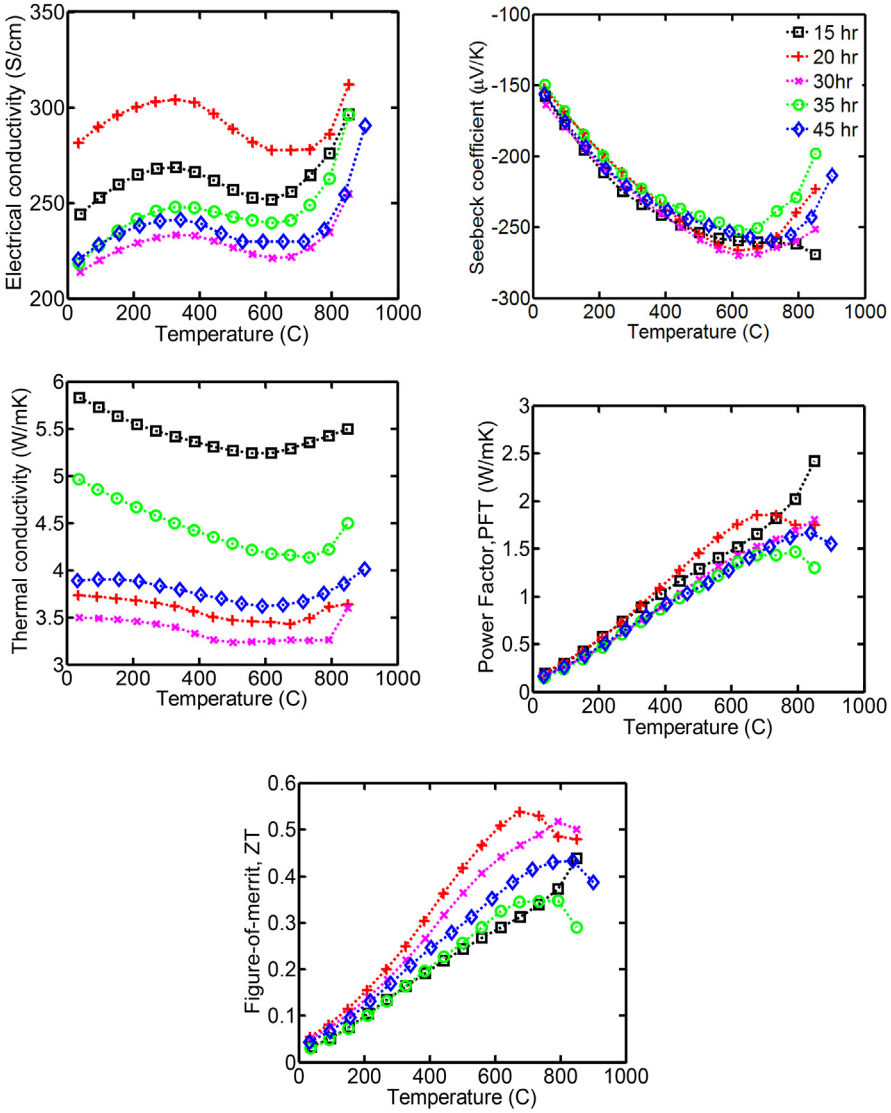

Fig. 6. Thermoelectric properties of sample 2 after annealing at 850 °C for 15, 20, 30, 35 and 45 h. The optimum annealing temperature is shown to be 20 h.

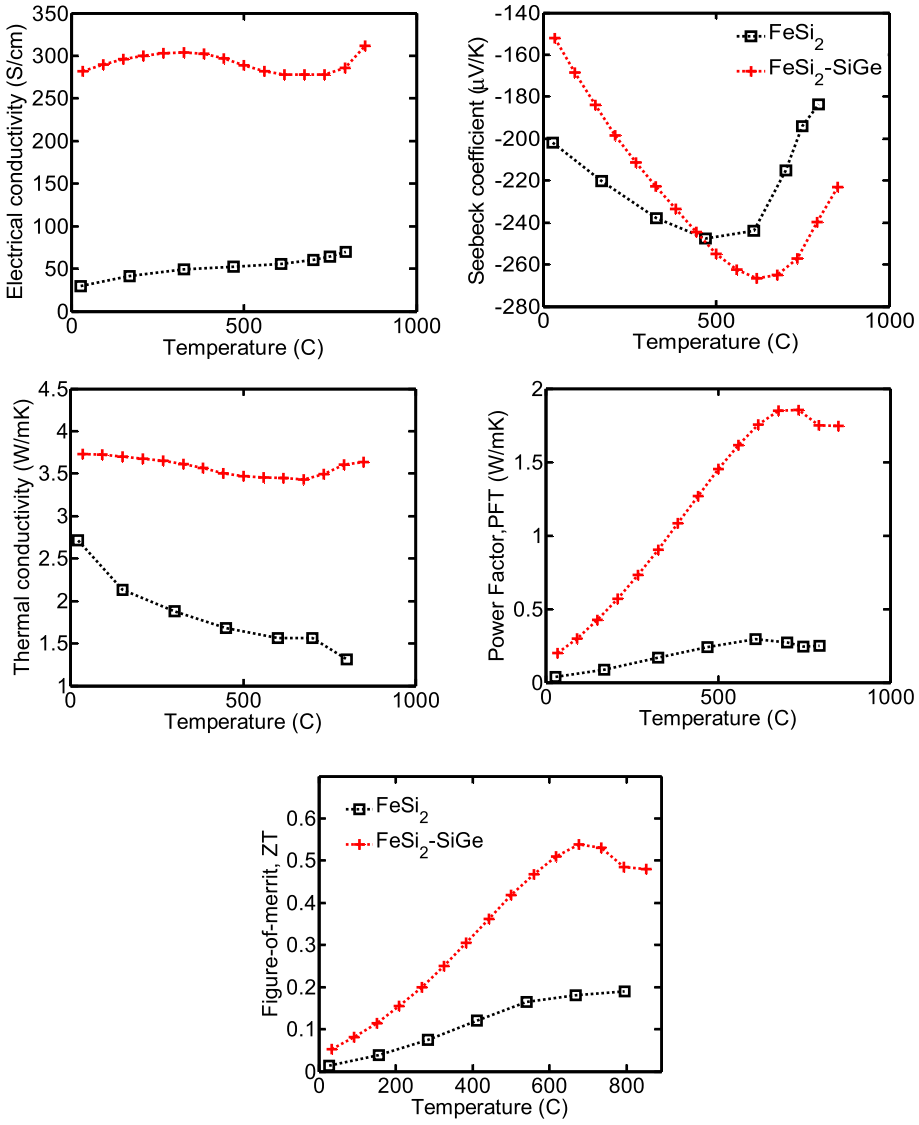

Fig. 7. Thermoelectric properties of hot-pressed $FeSi_2$ and $FeSi_2$-SiGe. The addition of SiGe to $FeSi_2$ significantly improved ZT.

of 500–850 °C, which makes it a material of choice for a wide range of applications in mid-to-high temperature.

Fig 7 shows the comparison of the thermoelectric properties of SiGe–$FeSi_2$ composite sample 2 and a single phase $FeSi_2$ sample prepared with similar hot-press conditions. It could be inferred from the diagrams that the inclusion of SiGe in the $FeSi_2$ matrix has increased the Seebeck coefficient at temperatures above 500 °C. The increase in electrical and thermal conductivity can be attributed to SiGe phase. The interplay of these effects concludes in a many times higher PFT, which results in a higher ZT for the composite system.

In the final trial, the thermoelectric properties of sample 2 after being annealed for 45 h at 850 °C were studied to find the maximum working temperature of the composite (Fig. 8). It could be seen that the composite is withstanding up to around 920 °C after which the transformation from beta thermoelectric phase to alpha metallic phase takes place. This transformation resulted in a sharp increase in both electrical conductivity and thermal conductivity along with a sharp decrease in Seebeck coefficient, which are the characteristics of a metallic phase material. As a result, the ZT dropped significantly after the phase transformation. The reverse phase transformation of α-$FeSi_2$ to β phase happens after a long-time annealing process as confirmed by annealing the sample for 15 h at 850 °C. The values of the electrical conductivity, Seebeck coefficient, and thermal conductivity were reproducible within the accuracy of the experiments.

4. Conclusion

The composite structure of $(FeSi_2)_{0.75}(SiGe)_{0.25}$ prepared by mechanical milling of the constituents elemental powders was investigated. Bulk samples were prepared using hot-press sintering with different conditions. The optimum annealing process was found. It was shown that the sample sintered at 1000 °C for 6 min under 120 Mpa pressure and annealed for 20 h at 850 °C had the highest ZT of 0.54, which was more than twice the ZT value of single phase $FeSi_2$ made under similar conditions. This composite system showed a ZT of above 0.4 for the entire temperature range of 500–850 °C which makes it a promising material for the mid-to-high temperature thermoelectric applications.

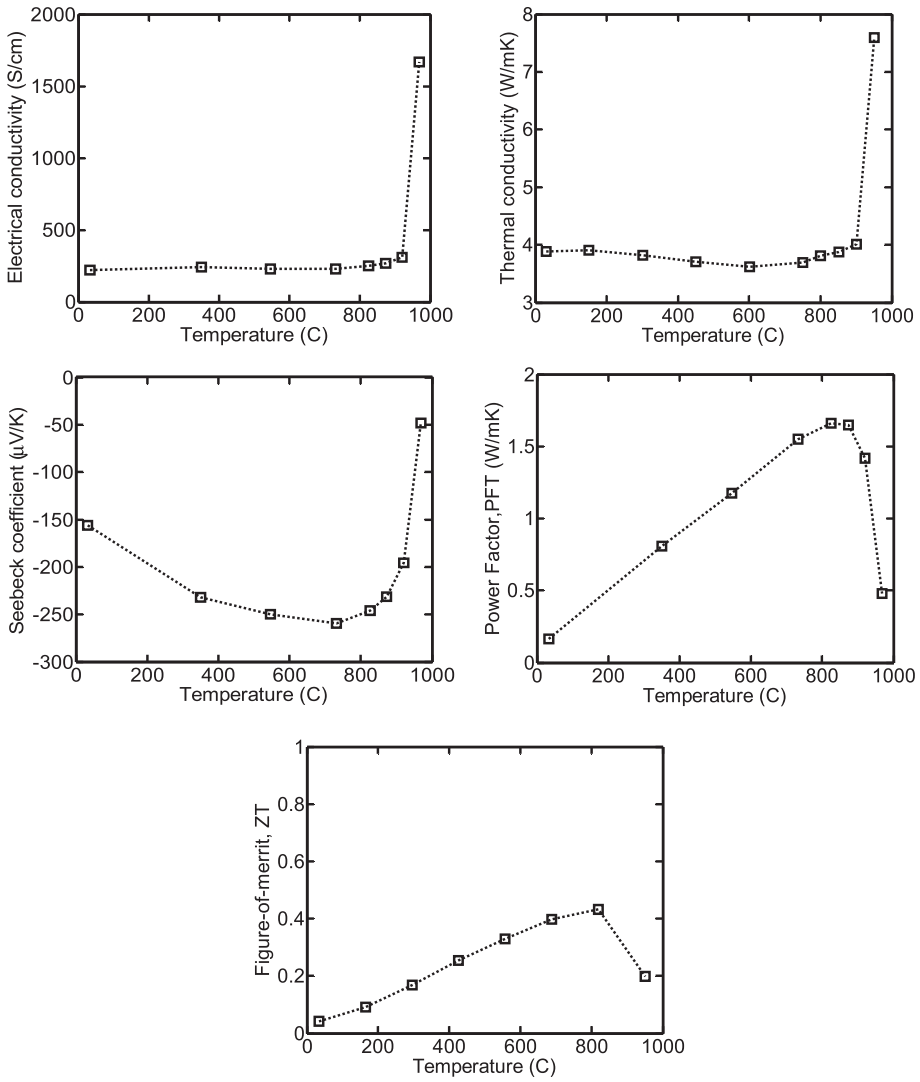

Fig. 8. Thermoelectric properties of sample 2 annealed at 45 h measured up to 980 °C. Maximum working temperature of the composite was found to be 920 °C.

Acknowledgments

This work was partially supported by Air Force Office of Scientific Research (AFOSR) under grant no. FA9550-10-1-0010 and the National Science Foundation (NSF) under grant numbers ECCS-1351533 and CMMI-1363485.

References

[1] Rowe DM. Thermoelectrics handbook: macro to nano. CRC Press; 2005.
[2] Christofferson J, Vashaee D, Shakouri A, Melese P. ASME, New York, NY. 2001. New York, NY.
[3] Fan Xiaofeng, Zeng Gehong, LaBounty Chris, Vashaee Daryoosh, Christofferson James, Shakouri Ali, et al. Proceedings of XX International Conference on Thermoelectrics (ICT). 2001. p. 405–8.
[4] Zhang Y, Vashaee D, Christofferson J, Zeng G, LaBounty C, Piprek J, et al. ASME Symp. Analysis applications heat pump refrigeration systems. 16–21 2003.
[5] Vashaee D, Zhang Y, Shakouri A, Zeng G, Chiu Y-J. Demonstration of electron filtering to increase the seebeck coefficient in In0.53Ga0.47As/In0.53Ga0.28Al0.19As superlattices. Phys Rev B Condens. Matter Mater Phys 2006;74:205335.
[6] Vashaee D, Zhang Y, Shakouri A, Zeng G, Chiu YJ. Phys Rev B 2006;74(19):195315.
[7] Mildred Dresselhaus, Gang Chen, Zhifeng Ren, Jean-Pierre Fleurial, Pawan Gogna, Ming Y Tang, Daryoosh Vashaee, Hohyun Lee, Xiaowei Wang, Giri Joshi, Gaohua Zhu, Dezhi Wang, Richard Blair, Sabah Bux, Richard Kaner. MRS Proceedings 1044(1).
[8] Satyala N, Vashaee D. Appl Phys Lett 2012;100(7). 073107–073107-4.
[9] Dehkordi AM, Vashaee D. Phys Status Solidi (a) 2012;209(11):2131–4.
[10] Satyala N, Vashaee D. J Appl Phys 2012;112(9):093716.
[11] Satyala N, Norouzzadeh P, Vashaee D. Nano bulk thermoelectrics: concepts, techniques, and modeling, nanoscale thermoelectrics. Springer International Publishing; 2014. p. 141–83.
[12] Vashaee D, Shakouri A. Microscale Thermophys Eng 2004;8(2):91–100.
[13] Vashaee D, Shakouri A. J Appl Phys 2007;101(5). 053719–053719-5.
[14] Vashaee D, Shakouri A. Improved thermoelectric power factor in metal-based superlattices. Phy Rev Lett 2004;92(10):106103-1–106103-4.
[15] Heremans JP, Jovovic V, Toberer ES, Saramat A, Kurosaki K, Charoenpakdee A, et al. Science 2008;32:554.
[16] Sumithra S, Takas NJ, Misra DK, Nolting WM, Poudeu PFP, Stokes KL. Enhancement in thermoelectric figure of merit in nanostructured Bi_2Te_3 with semimetal nanoinclusions. Adv Energy Mater 2011;1:1141–7.
[17] Zamanipour Zahra, Vashaee Daryoosh. J Appl Phys 2012;112:093714.
[18] Satyala N, Rad AT, Zamanipour Z, Norouzzadeh P, Krasinski JS, Tayebi L. J Appl Phys 2014;115(4):044304.
[19] Satyala N, Rad AT, Zamanipour Z, Norouzzadeh P, Krasinski JS, Tayebi L. J Appl Phys 2014;115(20):204308.
[20] Norouzzadeh P, Myles CW, Vashaee D. J Phys Condens Matter 2013;25(47):475502.
[21] Snyder GJ, Toberer ES. Complex thermoelectric materials. Nat Mater 2008;7(2):105–14. http://dx.doi.org/10.1038/nmat2090.
[22] Norouzzadeh P, Myles CW, Vashaee D. J Appl Phys 114(16):163509.
[23] Norouzzadeh P, Zamanipour Z, Krasinski JS, Vashaee D. J Appl Phys 2012;112(12):124308–124308–7.

[24] Satyala N, Vashaee D. J Electron Mater 2012;41(6):1785–91.
[25] Nozariasbmarz A, Tahmasbi Rad A, Zamanipour Z, Krasinski JS, Tayebi L, Vashaee D. Scr Mater 2013;69(7):549–52.
[26] Zamanipour Z, Shi X, Mozafari M, Krasinski JS, Tayebi L, Vashaee D. Ceram Int 2013;39(3).
[27] Zamanipour Z, Salahinejad E, Norouzzadeh P, Krasinski JS, Tayebi L. J Appl Phys 2013;114(2):023705.
[28] Ware RM, McNeill DJ. Iron disilicide as a thermoelectric generator material. Electr Eng Proc Institution 1964;111(1):178–82.
[29] Heinrich A, Griessmann H, Behr G, Ivanenko K, Schumann J, Vinzelberg H. Thermoelectric properties of β-$FeSi_2$ single crystals and polycrystalline β-$FeSi_2$+x thin films. Thin Solid Films 2001;381(2):287–95.
[30] Chen HY, Zhao XB, Stiewe C, Platzek D, Mueller E. Microstructures and thermoelectric properties of co-doped iron disilicides prepared by rapid solidification and hot pressing. J Alloys Compd 2007;433(1–2):338–44.
[31] Meng QS, Fan WH, Chen RX, Munir ZA. Thermoelectric properties of nanostructured $FeSi_2$ prepared by field-activated and pressure-assisted reactive sintering. J Alloys Compd 2010;492(1–2):303–6.
[32] Qu X, Lü S, Hu J, Meng Q. Microstructure and thermoelectric properties of β-$FeSi_2$ ceramics fabricated by hot-pressing and spark plasma sintering. J Alloys Compd 2011;509(42):10217–21.
[33] Kim SW, Cho MK, Mishima Y, Choi DC. High temperature thermoelectric properties of p- and n-type β-$FeSi_2$ with some dopants. Intermetallics 2003;11(5):399–405.
[34] Ito M, Nagai H, Katsuyama S, Majima K. Effects of Ti, Nb and Zr doping on thermoelectric performance of β-$FeSi_2$. J Alloys Compd 2001;315(1–2):251–8.
[35] Tani J-i, Kido H. Mechanism of electrical conduction of Mn-doped beta-$FeSi_2$. J Appl Phys 1999;86(1):464–7.
[36] Chen HY, et al. Influence of nitrogenizing and Al-doping on microstructures and thermoelectric properties of iron disilicide materials. Intermetallics 2005;13(7):704–9.
[37] Poudel B, et al. High-thermoelectric performance of nanostructured bismuth antimony telluride bulk alloys. Science 2008;320(5876):634–8.
[38] Sugihara S, Morikawa K. Improved thermoelectric performances of oxide-containing $FeSi_2$. Mater Trans 2011;52(8):1526–30.
[39] Ito M, Tada T, Katsuyama S. Thermoelectric properties of $Fe_{0.98}Co_{0.02}Si_2$ with ZrO_2 and rare-earth oxide dispersion by mechanical alloying. J Alloys Compd 2003;350(1–2):296–302.
[40] Ito M, Nagai H, Tanaka T, Katsuyama S, Majima K. Thermoelectric performance of n-type and p-type β-$FeSi_2$ prepared by pressureless sintering with Cu addition. J Alloys Compd 2001;319(1–2):303–11.
[41] Yamauchi I, Ueyama S, Ohnaka I. β-$FeSi_2$ phase formation from a unidirectionally solidified rod-type eutectic structure composed of both α and ε phases. Mater Sci Eng A 1996;208(1):108–15.
[42] Das A, Manna I, Pabi SK. A numerical model of peritectoid transformation. Metallurgical Mater Trans A 1999;30(10):2563–73.
[43] Dismukes JP, Ekstrom L, Steigmeier EF, Kudman I, Beers DS. Thermal and electrical properties of heavily doped Ge-Si alloys up to 1300 °K. J Appl Phys 1964;35(10):2899–907.
[44] Slack GA, Hussain MA. The maximum possible conversion efficiency of silicon-germanium thermoelectric generators. J Appl Phys 1991;70(5):2694–718.
[45] Rowe DM. CRC handbook of thermoelectrics. Boca Raton, FL: CRC; 1995.
[46] Joshi G, et al. Enhanced thermoelectric figure-of-merit in nanostructured p-type silicon germanium bulk alloys. Nano Lett 2008;8(12):4670–4.
[47] Wang XW, et al. Enhanced thermoelectric figure of merit in nanostructured n-type silicon germanium bulk alloy. Appl Phys Lett 2008;93(19):193121–3.
[48] Zamanipour Z, Shi X, Dehkordi AM, Krasinski JS, Vashaee D. Phys Status Solidi (a) 2012;209(10):2049–58.
[49] Zamanipour Z, Krasinski JS, Vashaee D. J Appl Phys 2013;113(14). 143715–143715-5.